

NANO AND BULK CRYSTALS OF ZnO: SYNTHESIS AND CHARACTERIZATION

Atul Gupta, H. S. Bhatti, D. Kumar, N. K. Verma^a, R. P. Tandon^b

Department of Physics, Punjabi University, Patiala-147 002, Punjab, India.
SPMS, Thapar Institute of Engineering and Technology, Patiala-147 004, Punjab, India.
Department of Physics, University of Delhi, Delhi, India.

Different sized (micro to nano) crystals of zinc oxide were obtained using different techniques of synthesis. Micro sized crystals were obtained by sintering zinc oxide with Di_2O_3 , B_2O_3 and V_2O_5 fluxes. For preparing nanocrystals, precursor was prepared from zinc acetate and absolute ethanol. X-ray diffraction patterns of the crystals were obtained which confirm the wurtzite crystal structure of the ZnO phosphors. Scanning electron microscopic and transmission electron microscopic images of the prepared samples were recorded from where the particle sizes of the various samples of ZnO were calculated to be varying from 7.8 nm to 3 mm. Synthesized single, micro- and nano-crystals of ZnO were excited by nitrogen laser. Time resolved hyperbolic decay curves were observed from where various optical parameters such as excited state life-times ranging from 190 ns to 25.30 μs , trap-depths varying from 0.14 eV to 0.27 eV and decay constant lying in between 0.56 to 0.72 were obtained.

Keywords: Single crystal, bulk crystal, nano crystal, ZnO, XRD, TEM, SEM.

1. Introduction

Zinc oxide is a very fast and efficient phosphor because of its wide band gap, large exciton binding energy and low threshold power for optical pumping [1-4]. PbO and PbF_2 fluxes were used to prepare single crystals of pure and doped zinc oxide by various workers who studied their optical and electrical properties [5-7]. Various chemical synthesis methods have been employed by several workers to synthesize nano / micro crystals such as solvothermal, hydrothermal, self assembly and sol-gel, etc [8-12]. Various workers have been working on synthesis and characterization of different nanostructures of pure and doped zinc oxide phosphors. Spanhel and Anderson have explained the synthesis of nano crystals of zinc oxide using distillation set-up starting with products of zinc acetate and ethanol [13]. Using this technique they have obtained highly concentrated colloidal nanocrystals of ZnO of size varying from 3.5 nm - 5.5 nm with ageing and shown that these crystals remain in a dispersed state for weeks. Hossain et al have further modified this technique successfully to obtain nanobelts of ZnO of length 700 μm using refluxing technique [14]. However our group has produced ZnO nanobelt of length 2.8 mm with increasing reaction time using the refluxing technique starting with zinc acetate and absolute ethanol [15]. Several workers have used capping agents such as poly vinyl pyridine (PVP), poly ethylene glycol (PEG) etc to stop particle agglomeration and obtained nanoparticles of size less than 5 nm [16-17]. These polymers produce spherical nanoparticles in shape because of the property of surface tension. Sol-gel and thin film deposition techniques are other best alternates to obtain particle size less than 5 nm [18-19]. Chakrabarti et al have obtained ZnO nanoparticles of size varying from 2.84 – 2.94 nm using tetraethylorthosilicate (TEOS) gel [19]. Figure 1 represents the brief review of various synthesis routes for preparing nanostructures of ZnO. This paper contributes for the synthesis and characterization of bulk- and nano-crystals of zinc oxide using various preparation routs. B_2O_3 , V_2O_5 and Di_2O_3 fluxes have been tried to improve the crystallinity of ZnO. Nanocrystals of ZnO have been prepared using Spanhel and Anderson method [13].

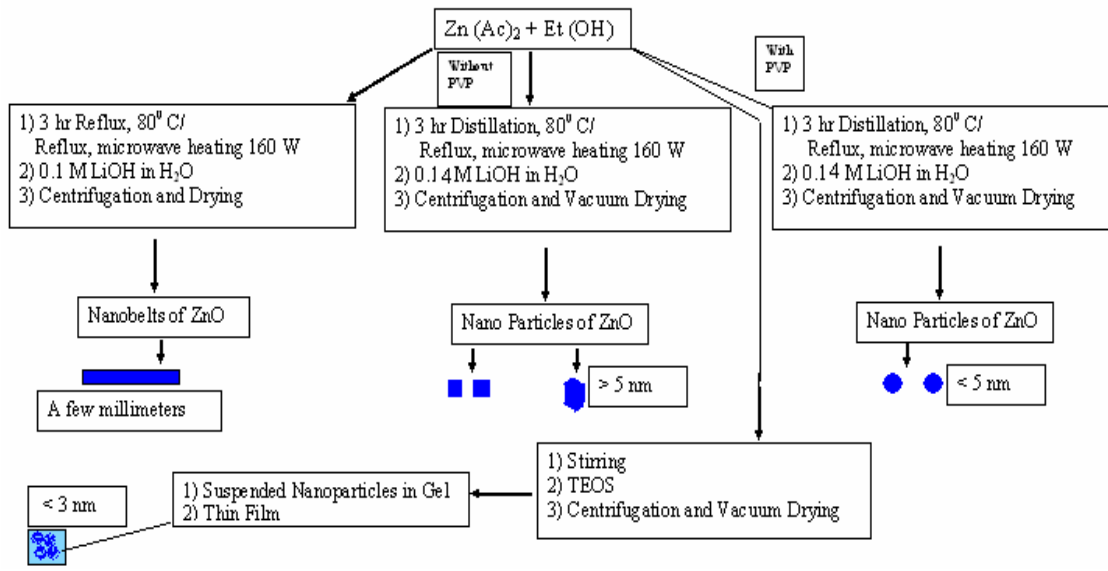


Fig. 1. Various Synthesis Routes for preparing Nanostructures of ZnO

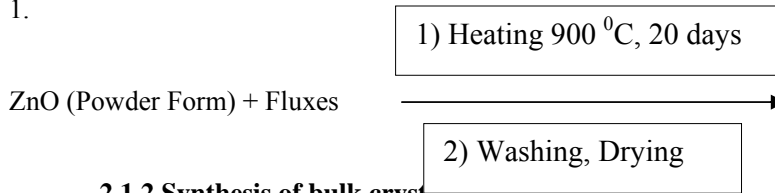
2. Synthesis and characterization

2.1 Synthesis of micro- and nano- crystals of ZnO

Various routes were tried for synthesis of single, micro and nano crystals of zinc oxide which are discussed in detail as follows:

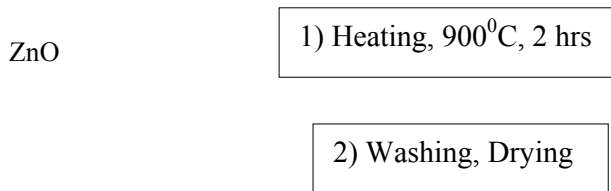
2.1.1 Synthesis of single crystal using B_2O_3 and V_2O_5 fluxes

Single crystals of zinc oxide have been synthesized using flux method. B_2O_3 and V_2O_5 have been used as fluxes to improve the crystallinity. The mixture of ZnO , B_2O_3 and V_2O_5 was kept in a furnace for twenty days at $900^\circ C$ in a platinum crucible. After which the crystals were washed with distilled water and dried in an oven for half an hour. This method will be named as synthesis method 1.



2.1.2 Synthesis of bulk crystals

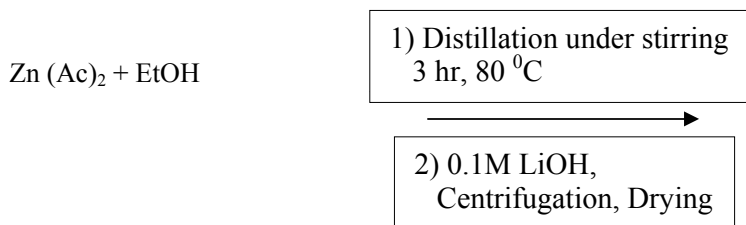
ZnO was sintered in air for two hours in a muffle furnace at $900^\circ C$. The sample was then crushed to fine powder form and washed with distilled water to remove the residual impurities and dried in an oven at a temperature $100^\circ C$ for half an hour. This method will be named as synthesis method 2.



2.1.3 Synthesis of micro-sized crystals using absolute ethanol

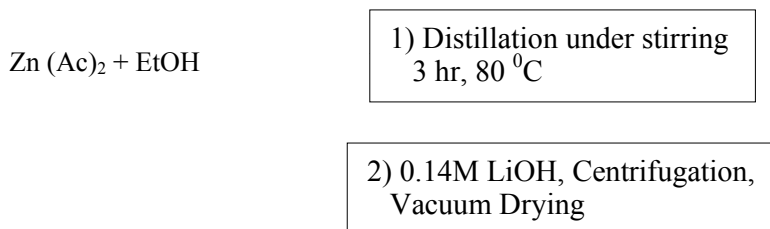
Colloidal solution was prepared from zinc acetate and absolute ethanol. $0.1M Zn^{2+}$ prepared from zinc acetate in absolute ethanol was refluxed under distillation and stirred for 3 hours at $80^\circ C$. This is initially based on the method given by Spanhel et al, 1991. Condensate was separated out. The remaining hygroscopic product was mixed with $0.1M LiOH$ prepared in $100ml$ deionized water in which precipitates started forming after then precipitates were separated out using centrifugal

machine at 2500 rpm. Sample was then dried in the oven in oxygen atmosphere at 150 °C. This method will be named as synthesis method 3.



2.1.4 Synthesis of nanocrystals using absolute ethanol

The precursor was prepared from zinc acetate and absolute ethanol in distillation set-up. 0.1M Zn²⁺ prepared from zinc acetate in absolute ethanol was refluxed under distillation and magnetic stirring for 3 hr at 80 °C. Condensate was separated out. The remaining hygroscopic product was mixed with 0.14M LiOH prepared in 100ml deionized water. Precipitates were separated out using centrifugal machine at 3500 rpm. Sample was then dried in the vacuum oven at 80 °C for 4 hours. The difference between this method and method mentioned in 2.1.3 is that the growth of nanocrystals is controlled with increasing molar concentration of LiOH from 0.1M to 0.14 M. By doing so the near neutral clusters are formed and pH values comes to be 8. Another change is in increased angular velocity of precipitates in centrifugal machine. This method will be named as synthesis method 4.



2.2 Characterization of micro- and nano- crystals of ZnO

2.2.1 Optical characterization

Nitrogen laser was employed for excitation of micro- and nano-crystals of zinc oxide. Nitrogen laser operates at wavelength of 337.1 nm (ultraviolet region) with high peak power 10 kW, pulsed in operation (7 ns). Synthesized crystals of ZnO were pasted on Pyrex glass plate using xylene. Emission was observed at an angle of 90° to the laser beam and the emission wavelength was selected by a monochromator. After selection of the emission wavelength, signal was sent to a photo-multiplier tube from where multiexponential decay curves were observed and finally sent to computer for simulation purposes. Absorption spectra of the micro- and nano-crystals of ZnO were obtained using Perkin Elmer spectrophotometer.

2.2.2 Morphological characterization

Micro sized crystals of zinc oxide have been studied using X-ray diffraction (XRD) pattern and scanning electron microscopy (SEM). Nanocrystals of ZnO are characterized using transmission electron microscopy (TEM) and XRD. X-ray Diffraction (XRD) data for structural characterization of the various prepared samples of ZnO were collected on an X-ray diffractometer (PW1710) using Cu-K α radiation. Scanning electron microscope (SEM) images of the samples were obtained from JSM-6100 type microscope. Transmission electron microscope (TEM) images of the samples were obtained using JEOL JEM 2000 Ex type microscope.

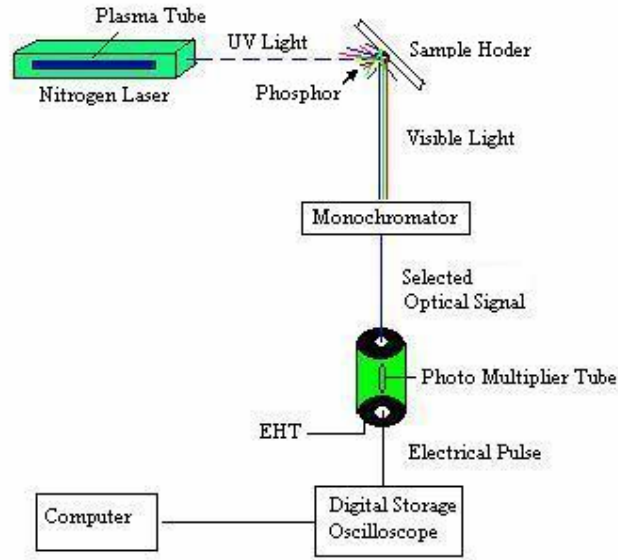


Fig. 2. Experimental Set-up using nitrogen laser as an excitation source. Emission wavelength is selected by monochromator. The decay curve is obtained by digital storage oscilloscope and simulated using computer assembly.

3. Theoretical

3.1 Theory of Luminescence

When samples are exposed to the laser radiation, the electrons are raised from valence band to excited states. These electrons may return to the valence band with the emission of characteristic luminescent radiation. Intensity of phosphorescence radiation 'I' at time 't' given by

$$I = I_0 e^{-pt}$$

straight line in case of single lifetime. However, in most of the cases, when one comes across the interaction of radiation with solids, there are trapping levels at different depths leading to multiple lifetime components yielding multiexponential decay curves. Transitions from the various radiative traps (trap-depths) corresponding to transition probability values are obtained from the following relation:

$$p = S e^{-E/kT}$$

where "E" is the energy of the level in the forbidden gap of the semiconductor (trap-depth), "S" is the escape frequency factor ($\sim 10^9 \text{ s}^{-1}$), "k" is the Boltzmann's constant and "T" is the absolute temperature .

In most of the cases, when one come across the interaction of radiation with solids, there are trapping levels at different depths. In an ideal case of uniform distribution, one can assume an equal number of traps at all depths. However in most of the cases, the distribution of traps, at different depths, is not uniform and is given by equation:

$$I = I_0 t^{-b}$$

where b is called the decay constant, a deciding factor for the distribution of trap states.

3.2 Particle size measurements

Particle size 'D' was calculated using Scherer formula

$$D = 0.9 \lambda / \beta \cos \theta$$

where λ is the wavelength of Cu-K α radiations (1.54Å), β full width at half maximum of the peak corresponding to plane <101> and θ is the angle obtained from 2θ value corresponding to maximum intensity peak in XRD pattern.

Energy band gap was calculated from the effective mass model, which is given as below

$$E = E_g + \frac{\pi^2 \hbar^2}{2m_0 R^2 \mu} - \frac{1.8e^2}{4\pi\epsilon_r R}$$

First term in the relation corresponds to band gap ($E_g = 3.37$ eV) of bulk crystals, second term is due to quantum confinement effects and third term is related with Coulomb interaction. R is the radius of the nanoparticles obtained from the XRD (average particle size = 7.8 nm). Equations (4) and (5) have been used to simulate particle size and band gap energy respectively of the ZnO nanocrystals using synthesis method 4.

4. Results and discussion

Different sized (micron to nanometer) crystals of zinc oxide phosphors have been synthesized using four different methods and their optical and morphological characterizations have been done using Time Resolved Laser Induced Photoluminescence (TRPL), X-ray Diffraction (XRD) analysis, Scanning Electron Microscopy (SEM) and Transmission Electron Microscopy (TEM) and UV absorption spectroscopy. Figure 2 represents the experimental set-up for photoluminescence multiexponential decay measurement using N_2 – laser as the excitation source. Figure 3 (a) represents the photograph of 3 millimeter sized crystal of zinc oxide using photogenic camera and (b) represents the XRD pattern of the crystal synthesized by method 1. Figure 4 (a) represents scanning electron microscopic image and (b) represents X-ray Diffraction pattern of the zinc oxide crystals synthesized by method 2. Figure 4 (a) reveals the crystal size varying from 1 - 4 μm of ZnO and figure 4 (b) of XRD pattern of ZnO confirms wurtzite crystal structure of the ZnO. Lattice constants ($a = b = 0.32$ nm and $c = 0.52$ nm) and diffraction peaks corresponding to the planes $\langle 100 \rangle$, $\langle 002 \rangle$ and $\langle 101 \rangle$ obtained from X-ray diffraction data are consistent with the JCPDS data of ZnO. Figure 5 represents the scanning electron microscopic image of the zinc oxide crystals obtained using synthesis method 3 and shows the crystal size less than 1 μm . Figure 6 represents the intensity vs. time graph for the crystals synthesized by method 1, 2 and 3 by curves a, b and c respectively. Figure 7 (a) represents the transmission electron microscopic image of the nanocrystals of ZnO and figure 7 (b) represents XRD pattern with broadened peaks of ZnO nanocrystals synthesized using method 4. TEM images reveals size of nanocrystals less than 10 nm and was confirmed using Scherer formula ($= 7.801$ nm) as obtained from XRD data. It is clear from the figure 8 that the life-time values of zinc oxide nanocrystals are in nano-second time domain. Figure 9 represents the absorption wavelength graph for micro- and nano-crystals of ZnO synthesized by method 3 and 4 respectively. Spectrum 1 in figure 9 shows the absorption peak at 364 nm for nanocrystals of ZnO as synthesized using method 4, whereas curve 2 indicate the absorption peak at 368 nm for microcrystals synthesized using method 3. It is clear from absorption spectroscopy that band gap increases on decreasing particle size. The band gap energy have also been confirmed using the effective mass (using equation 5) model with particle size 7.8 nm (using equation 4) as obtained from XRD data. Table 1 indicates the data of life-time, trap-depth and decay constant values of the micro- and nano-crystals. It is observed from the data that life-time and trap-depth values are decreasing as the particle size is decreasing. However decay constant values are increasing with decrease in particle size indicating the traps to be more uniform at nanolevel.

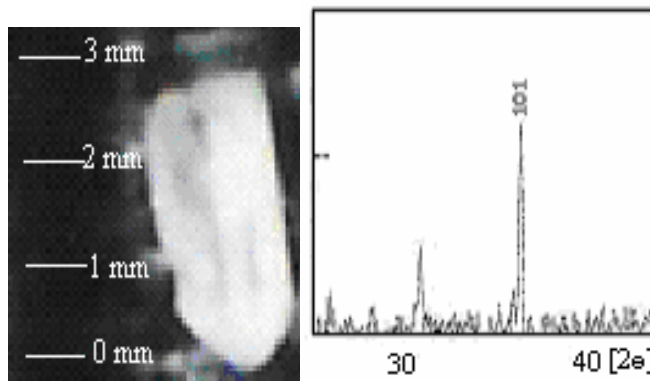


Fig. 3 (a) Photographs using photogenic camera and (b) X-Ray Diffraction (XRD) of Single Crystals of Zinc Oxide Synthesized by Method 1.

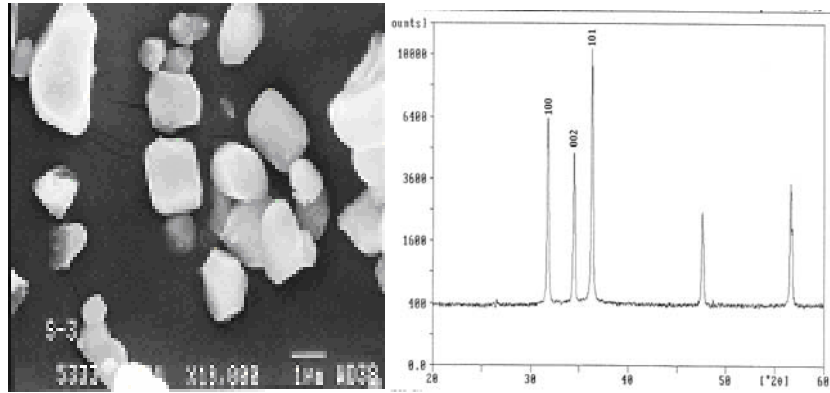


Fig. 4 (a) Scanning Electron Micrographs (SEM) and (b) X-ray Diffraction (XRD) Zinc Oxide Crystals Synthesized by Method 2.

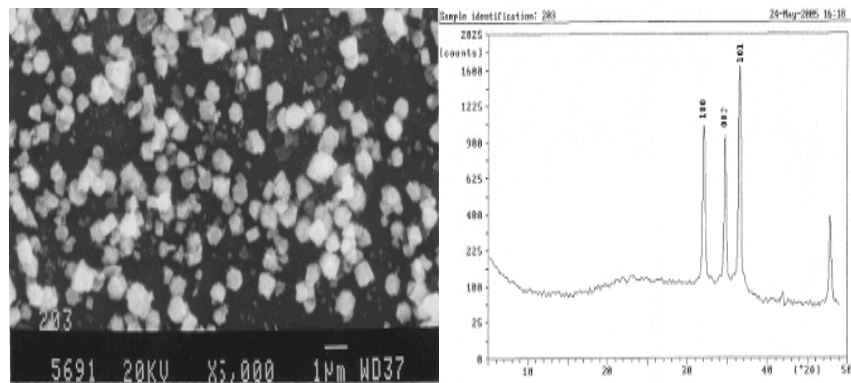


Fig. 5 (a) Scanning Electron Micrographs (SEM) and (b) X-ray Diffraction (XRD) of Zinc Oxide Crystals Synthesized by Method 3.

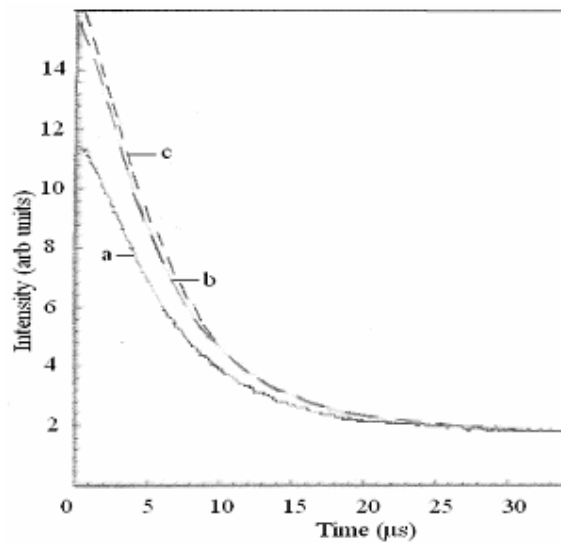


Fig. 6 Intensity vs. Time graph for the micro-crystal of ZnO synthesized by methods 1 (curve a), 2 (curve b) and 3 (curve c).

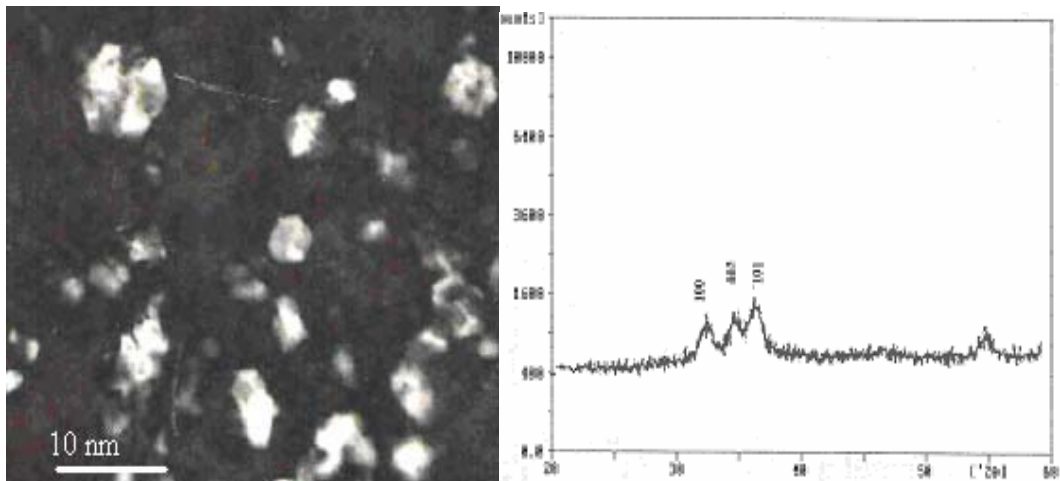


Fig. 7 (a) Transmission Electron Microscope (TEM) Image (b) X-ray Diffraction (XRD) for nanocrystals of Zinc Oxide synthesized by Method 4.

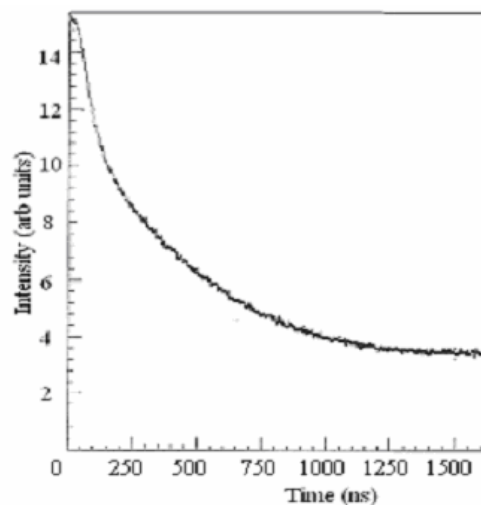


Fig. 8 Intensity vs. Time graph for nano-crystal of ZnO synthesized by method 4.

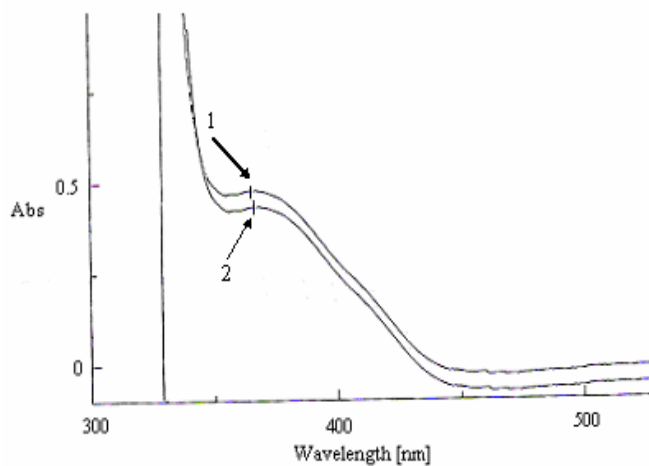


Fig. 9 Absorption Intensity vs. wavelength graph for ZnO nano-crystals (curve 1) and micro-crystals (curve 2) synthesized by method 4 and 3 respectively.

Table 1 Life-Time, Trap-Depth and Decay Constant Values for Micro- and Nano-Crystals of ZnO.

Sample synthesized by	Life-time values (in μs)			Trap-depth values (in eV)			Decay constant
	τ_1	τ_2	τ_3	E_1	E_2	E_3	
Method 1	8.04	13.56	25.30	0.24	0.25	0.27	0.56
Method 2	6.52	10.02	18.68	0.23	0.24	0.26	0.58
Method 3	6.24	10.38	22.36	0.23	0.24	0.27	0.62
Method 4	190*	8.72	15.74	0.14	0.24	0.26	0.72

*life-time values are in nanoseconds time domain

5. Conclusion

Micro- and nano-crystals of ZnO have been synthesized using different techniques and were characterized using XRD, SEM, TEM and TRPL. XRD pattern indicate the crystalline nature of the ZnO. Scanning electron microscopic and transmission electron microscopic images of the zinc oxide obtained indicate the size of the various crystals. It is concluded from time resolved laser induced photoluminescence spectra that the life-time values are varying from micro to nanoseconds and there is a considerable decrease in life-time values of the excited states. It is observed that with decreasing particle size of ZnO, life-time values are also decreasing and are in the order of nanosecond time domain for nanocrystals. Decay constant value for ZnO nanocrystals is highest among all the synthesized crystals. This indicates that the energy levels are more uniform within the energy band gap of the semiconductor material. Life-time shortening and increase in decay constant value of ZnO nanocrystals reveal that the synthesized nanophosphors are very efficient and fast. These synthesized crystals have various industrial applications such as active medium for laser oscillations, luminescent material for fluorescent tubes, bio-sensors etc.

Acknowledgements

This work has been supported by University Grants Commission, New Delhi Project No: 31-19/2005 (SR). The authors are also acknowledged to RSIC (XRD and SEM wing) Punjab University, Chandigarh for providing XRD pattern and SEM images.

References

- [1] Z. K. Yang, P. Yu, G. K. L. Wong, M. Kawasaki, A. Ohtomo, H. Koinuma and Y. Segawa, *Solid State Comm.*, **103**, 459, 1997.
- [2] D. M. Bagnall, Y. F. Chen, Z. Zhu, T. Yao, S. Koyama, M. Y. Shen and T. Goto, *Appl. Phys. Lett.*, **70**, 2230, 1997.
- [3] M. Kawasaki, A. Ohtomo, I. Ohkubo, H. Koinuma, Z. K. Tang, P. Yu, G. K. L. Wong, B. P. Zhang and Y. Segawa, *Sci. Engg.*, B **56**, 239, 1998.
- [4] A. Ohtomo, M. Kawasaki, I. Ohkubo, H. Koinuma, T. Yasuda and Y. Segawa, *Appl. Phys. Lett.*, **75**, 980, 1999.
- [5] N. Ohashi, T. Sekiguchi, K. Aoyama, T. Ohgaki, Y. Terada, I. Sakaguchi, T. Tsurumi and H. Haneda, *J. Appl. Phys.*, **91**, 3658, 2002.
- [6] N. Ohashi, J. Tanaka, T. Ohgaki, H. Haneda, M. Ozawa and T. Tsurumi, *J. Mat. Res.*, **17**, 1529, 2002.
- [7] N. Ohashi, T. Ohgaki, T. Nakata, T. Tsurumi, T. Sekiguchi, H. Haneda, J. Tanaka, *J. Korean Phys. Soc.* **35**, 287, 1999.
- [8] B. B. Lakshmi, C. J. Patrissi and C. R. Martin, *Chem. Mater.*, **9**, 2544, 1997.
- [9] L. Vayssieres, K. Keis, A. Hagfeldt and S. E. Lindquist, *Chem. Mater.*, **13**, 4395, 2001.
- [10] C. Pacholski, A. Kornowski, H. Weller, *Angew. Chem. Int. Edn. Engl.*, **41**, 1188, 2002.
- [11] L. Vayssieres, *Adv. Mater.*, **15**, 464, 2003.
- [12] B. Liu and H. C. Zeng, *J. Am. Chem. Soc.*, **125**, 4430, 2003.
- [13] L. Spanhel and M. R. Anderson, *J. Am. Chem. Soc.*, **113**, 2826, 1991.

- [14] M. K. Hossain, S. C. Ghosh, Y. Boontongkong, C. Thanachayanont and J. Dutta, *J. Meta. Nanocrys. Mat.*, **23**, 27, 2005.
- [15] H. S. Bhatti, A. Gupta, N. K. Verma and S. Kumar, *J. Mat. Sci: Mater Electron*, **17**, 281, 2006.
- [16] T. Hirano, H. Kozuka, *J. Mat. Sci.*, **38**, 4203, 2003.
- [17] A. Vladimir, Fonoberov and A. A. Balandina, *Appl. Phys. Lett.*, **85**, 24, 2004.
- [18] H. J. Lee, B. S. Kim, C. R. Cho and S. Y. Jeong, *Phys. Stat. Sol. (b)* **241**, 1533, 2004.
- [19] S. Chakrabarti, D. Ganguli and S. Chaudhuri, *J. Phys. D: Appl. Phys.* **36**, 146, 2003.
- [20] H. S. Bhatti, R. Sharma, N. K. Verma and S. Kumar, *Ind. J. Engg. Mat. Sc.*, **11**, 121, 2004.
- [21] H. S. Bhatti, A. Gupta, N. K. Verma and S. Kumar, *J. Phys. Chem. Solid*, **67**, 868, 2006.